Behavioral/Cognitive

Neural Responses to Heartbeats Detect Residual Signs of Consciousness during Resting State in Postcomatose Patients

Diego Candia-Rivera,[1]* Jitka Annen,[2,3]* Olivia Gosseries,[2,3] Charlotte Martial,[2,3] Aurore Thibaut,[2,3] Steven Laureys,[2,3#] and Catherine Tallon-Baudry[1#]

[1]Laboratoire de Neurosciences Cognitives et Computationnelles, Département d'Etudes Cognitives, École Normale Supérieure, INSERM, Université PSL, 75005 Paris, France, [2]GIGA-Consciousness, Coma Science Group, University of Liège, 4000 Liège, Belgium, and [3]Centre du Cerveau[2], University Hospital of Liège, 4000 Liège, Belgium

The neural monitoring of visceral inputs might play a role in first-person perspective (i.e., the unified viewpoint of subjective experience). In healthy participants, how the brain responds to heartbeats, measured as the heartbeat-evoked response (HER), correlates with perceptual, bodily, and self-consciousness. Here we show that HERs in resting-state EEG data distinguishes between postcomatose male and female human patients ($n = 68$, split into training and validation samples) with the unresponsive wakefulness syndrome and in patients in a minimally conscious state with high accuracy (random forest classifier, 87% accuracy, 96% sensitivity, and 50% specificity in the validation sample). Random EEG segments not locked to heartbeats were useful to predict unconsciousness/consciousness, but HERs were more accurate, indicating that HERs provide specific information on consciousness. HERs also led to more accurate classification than heart rate variability. HER-based consciousness scores correlate with glucose metabolism in the default-mode network node located in the right superior temporal sulcus, as well as with the right ventral occipitotemporal cortex. These results were obtained when consciousness was inferred from brain glucose met`abolism measured with positron emission topography. HERs reflected the consciousness diagnosis based on brain metabolism better than the consciousness diagnosis based on behavior (Coma Recovery Scale-Revised, 77% validation accuracy). HERs thus seem to capture a capacity for consciousness that does not necessarily translate into intentional overt behavior. These results confirm the role of HERs in consciousness, offer new leads for future bedside testing, and highlight the importance of defining consciousness and its neural mechanisms independently from behavior.

Key words: cerebral glucose metabolism; disorders of consciousness; heart rate variability; heartbeat-evoked response; random forests

Significance Statement

Detecting consciousness without relying on either overt behavior or asking to mentally perform a specific task is both a fundamental issue pertaining to the nature of consciousness and a clinical challenge. Here we show that the transient brain response elicited at each heartbeat captures residual consciousness in the resting-state EEG of postcomatose patients. The results show that brain responses to an internal bodily signal might help specify the gray zone of consciousness (i.e., the fleeting conscious feelings that are not necessarily associated with the performance of a specific task or translate into behavioral outputs).

Introduction

We recently proposed that the neural monitoring of signals ascending from the heart and gastrointestinal tract plays an important role in consciousness (Park and Tallon-Baudry, 2014; Tallon-Baudry et al., 2018; Azzalini et al., 2019). Visceral inputs are intrinsically private and might thus be self-specifying. More precisely, the neural responses to visceral inputs would contribute to conscious experience through first-person perspective, or to the bodily centered viewpoint from which we subjectively experience both the environment and inner mental life (Blanke and Metzinger, 2009). This represents a core component of the simplest, but also most elusive, aspect of consciousness. A number of experimental results in healthy adult participants support this hypothesis. How the brain transiently responds to heartbeats can be experimentally measured by averaging EEG or MEG data time locked to heartbeats, to generate the heartbeat-evoked response (HER; Schandry et al., 1986). In healthy participants, HERs predict perceptual consciousness (Park et al., 2014; Al et al., 2020), and reflect bodily consciousness (Park et al., 2016; Sel et al., 2017) and the self-versus-other distinction (Babo-Rebelo et al., 2019). HERs also covary with the self-relatedness of spontaneous thoughts, as rated by participants themselves (Babo-Rebelo et al., 2016a,b), suggesting that HERs do capture a component of consciousness not related to task performance. We thus hypothesized that heartbeat-evoked responses and their fluctuations could be a marker of consciousness even in the absence of overt behavior or mental response to instructions in the resting-state EEG of postcomatose patients with disorders of consciousness.

Probing consciousness in the absence of overt behavior is theoretically motivated but remains an experimental and clinical challenge. Consciousness is defined by the existence of subjective experience and inner mental life (Chalmers, 1995; Block, 2005), which does not necessarily translate into overt behavior (Tsuchiya et al., 2015)—in other words, subjective experience is necessary for consciousness while overt behavior is not. It follows that experimental work should focus on the neural mechanisms giving rise to conscious experience, rather than on the cognitive processes required for report in healthy participants (Frässle et al., 2014). In clinical practice, the threshold for unconsciousness/consciousness is currently placed between patients showing eye opening but only reflex-like responses to the environment [unresponsive wakefulness syndrome (UWS); Laureys et al., 2010] and patients with fluctuating but reproducible signs of nonreflex behavior [minimally conscious state (MCS); Giacino et al., 2002]. The clinical rationale is thus based solely on behavioral signs of consciousness (Bayne et al., 2017). In addition to the criticisms raised above, measuring consciousness from behavior is an issue in patients who might experience motor, sensory, or cognitive deficits, or in patients lacking the motivation or attentional resources to respond to the command. Consciousness indices that are based on brain activity and that do not require patients' active participation, such as neural responses to magnetic stimulation applied transcranially (Casali et al., 2013; Casarotto et al., 2016) or cerebral glucose metabolism at rest obtained with fluorodeoxyglucose (FDG) positron emission tomography (PET; Tommasino et al., 1995; Rudolf et al., 1999; Laureys et al., 2004; Nakayama et al., 2006; Thibaut et al., 2012; Gosseries et al., 2014; Stender et al., 2014, 2015), have been developed and validated. While behavioral assessments remain the clinical standard (Giacino et al., 2018; Kondziella et al., 2020), brain imaging provides complementary information in patients without command following FDG-PET, and is recommended by the European Academy of Neurology (Kondziella et al., 2020). In particular, FDG-PET seems useful to detect residual consciousness, or predict potential for consciousness recovery, from brain metabolism in patients without any behavioral sign of consciousness (Stender et al., 2014).

We tested whether HERs could reliably detect residual consciousness in postcomatose patients with disorders of consciousness using resting-state high-density EEG data ($n = 68$; training sample $n = 38$; validation sample $n = 30$; Table 1). To probe consciousness independently from behavior, we used the neuroimaging diagnosis of consciousness based on resting-state brain glucose uptake obtained with FDG-PET. EEG was measured during the FDG uptake phase. We further explored cases where the PET-based diagnosis was not congruent with the behavioral diagnosis, obtained from repeated standardized clinical assessments using the Coma Recovery Scale-Revised (CRS-R; (Giacino et al., 2004; Wannez et al., 2017).

Materials and Methods

Patients. Patients included in this study were referred to the University Hospital of Liège between January 2008 and October 2015 for a 1 week assessment of their state of consciousness. This included the acquisition of resting-state FDG-PET, high-density EEG data, and CRS-R assessments.

Included patients presented with a prolonged (at least 28 d) disorder of consciousness after severe brain damage, based on international guidelines and repeated CRS-R assessments (Giacino et al., 2018). Exclusion criteria were being underage or having pre-existing psychological or neurologic diseases, using sedative drugs, or FDG-PET and EEG contraindications. For the purpose of the present study, we trained classifiers on the consciousness diagnosis based on the assessment of FDG-PET data, hereafter termed PET-based diagnosis, as in the study by Stender et al. (2014). More details on the PET-based diagnosis are provided in the PET data and correlation with consciousness scores section. Similar analyses were performed using the clinical diagnosis based on the best assessment with the CRS-R of at least five assessments (Wannez et al., 2017), hereafter termed CRS-R diagnosis. The CRS-R assessment is based on at least five assessments performed on separate days within the 1 week hospitalization, including one CRS assessment systematically performed just before PET-EEG data acquisition. The assessment with the highest indication for consciousness, or best diagnosis, is retained for final CRS-R diagnosis (Wannez et al., 2017). The consistency of the CRS-R diagnosis corresponds to the percentage of sessions where the patient reaches his/her highest indication for consciousness. In the present dataset, the mean percentage of consistency across patients was 63 ± 4% SEM. Within the subgroup of patients where FDG-PET analysis indicated MCS but CRS-R indicated UWS [nonbehavioral MCS (MCS*)], the consistency of CRS-R assessments was 100%.

A total of 129 patients were included in the study. As detailed in the Results subsection Extracting the electrocardiogram from EEG data (independent component analysis derived from electrocardiogram), data from 61 patients had to be discarded from further analysis because it was not possible to extract 5 min of good-quality electrocardiogram from their EEG data. The final analysis of EEG data thus included 68 patients (Table 1, demographic information).

The study was approved by the ethics committee of the University Hospital of Liège. Patients' legal guardians gave written informed consent for approval of participation in the study, as required by the Declaration of Helsinki.

Data acquisition. FDG-PET data were acquired as described previously (Stender et al., 2014). In short, the patients fasted for at least 6 h before commencing the PET procedure. Patients remained in a dark room for ~10 min before and 30 min after injection of 150–300 mBq FDG, after which the PET was acquired. Patients were in resting state with eyes open. They were aroused when necessary following the same arousal facilitation protocol as used for CRS-R assessment (Giacino et al., 2004).

Table 1. Demographic information of patients included in the analysis

Group	PET diagnosis	Patients (females), n	Mean age (range), years	Mean since onset (range), months	Etiology
Training	MCS	31 (13)	41 (18–73)	33 (1–157)	TBI = 17, anoxia = 8, mix = 1, hemorrhage = 5
	UWS	7 (2)	44 (28–65)	23 (3–66)	TBI = 1, anoxia = 4, mix = 1, hemorrhage = 1
Validation	MCS	24 (13)	38 (22–70)	25 (2–118)	TBI = 9, anoxia = 9, mix = 1, hemorrhage = 2, infection = 2, hypoglycemia = 1
	UWS	6 (2)	47 (32–65)	35 (1–168)	Anoxia = 5, hemorrhage = 1
Total		68 (30)	38 (18–73)	30 (1–168)	

TBI, Traumatic brain injury.

EEG was recorded during the FDG uptake phase (i.e., after FDG injection, but before tomography began). High-density EEG recordings were obtained from 256 scalp sensors using saline electrode nets designed by Electric Geodesics, with a sampling rate of 250 or 500 Hz. EEG recordings were performed during the dark period of the FDG-PET protocol (i.e., ~10 min before until 30 min after the FDG injection). The EEG net was removed before the PET scan was performed. In eight patients, and 5 additional healthy control subjects, an electrocardiogram (EKG) was obtained from electrodes placed below the left and right clavicles using the Polygraph Input Box (Electric Geodesics).

EEG data preprocessing. EEG preprocessing was performed using the Fieldtrip toolbox (Oostenveld et al., 2011) in MATLAB R2016b. Data were downsampled from 500 to 250 Hz, when applicable, and offline filtered (1–25 Hz Butterworth bandpass filter with a Hamming windowing at cutoff frequencies), and z scores per channel over time were calculated.

The first step in data analysis was to identify a 5 min time window of a good-quality EEG, where chances to derive an EKG from EEG data would be maximized. In each candidate 5 min time window, we quantified noise as the total duration of EEG segments exceeding a z-scored amplitude of 20, across all channels. In each of the 129 patients, the least noisy 5 min time window was retained for further analysis.

Within the selected 5 min time window, we then identified channels with artifacts. We computed the area under the curve (AUC) of the z-score amplitude during the selected 5 min for each channel and examined the distribution across channels. Channels exceeding +3 SDs of the AUC distribution for all channels were discarded (77 ± 4 SEM channels rejected on average, most often located over cheeks and neck). This procedure was iterated until all channels satisfied the +3 SD criterion or >50 channels had to be discarded, at which point the participant would be excluded from further analysis, a case that did not occur in the present dataset. To further identify bad channels, we computed the correlation between each channel and its neighbors to identify channels with low correlation, indicative of artifacts such as poor contact. Neighborhood relationships were computed using the default neighborhood definition in Fieldtrip considering neighbors' channels up to distances of 4 cm. For each channel, we computed a mean correlation score corresponding to the mean correlation with neighbors, weighted by the distance between channels. Channels with a weighted-by-distance correlation <60% were replaced by spline interpolation of neighbors.

After independent component analysis (ICA) correction (see below for details), we restricted the analysis to the 175 channels located on the scalp, excluding channels on face and neck. Finally, the EEG dataset was rereferenced using a common average (Candia-Rivera et al., 2020a,b) and reduced to the same 64 channel set in each patient, corresponding to standard scalp locations in the 10–10 system (Luu and Ferree, 2000).

Extracting the electrocardiogram from EEG data (independent component analysis derived from electrocardiogram). EEG electrodes measure brain activity but also electrical cardiac activity. This is known as the cardiac artifact (Dirlich et al., 1997). It follows that it is possible to recover the EKG from scalp EEG data (Raimondo et al., 2017). To extract the EKG from EEG, we used ICA to obtain ICA-corrected EEG data on the one hand and an electrocardiogram derived from ICA (ICA-EKG) on the other hand. This procedure was successful in 68 patients. Of 129 patients, 61 were discarded at the ICA-EEG stage, 50 because ICA-EKG extraction was not successful, and 11 because artifact-free ICA-EKG could not be obtained in 5 min of continuous recordings.

We obtained the independent components using the "ICA extended" algorithm (Jung et al., 1998). The ICA component showing heart-induced activity with the clearest R peaks, and a gradient ear-to-ear amplitude topography (Dirlich et al., 1997) was selected for further analysis. If the R peaks were not clear in part of the 5 min segment, we selected a new 5 min segment, and performed the whole preprocessing again starting from the rejection of bad channels onward. ICA components related to cardiac activity were removed from EEG signals. The output of this procedure is thus a 5 min segment of EEG data ICA corrected for the cardiac artifact, and a corresponding 5 min segment of ICA-EKG (i.e., the electrocardiogram extracted by ICA from the EEG data).

R peaks were detected on the ICA-EKG using an automated process. First, a time window containing at least 5 R peaks with good signal-to-noise ratio was manually selected. Epochs from 400 ms before to 400 ms after each of those five R peaks were averaged to generate a heartbeat template specific to each patient. The template was then correlated with the entire EKG signal to automatically detect the R peaks. The local maxima of the correlation, indicating the presence of a heartbeat, were detected over the whole 5 min EKG data, in sliding time windows of a duration equal to the mean interbeat intervals duration obtained in the template plus 200 ms, computed at each sample. To limit the number of false-positive results, consecutive detected peaks separated by a duration smaller than the estimated mean interbeat interval duration minus 200 ms were discarded automatically. Both peak detection and the resulting histogram of interbeat interval duration were visually inspected in each patient, and manual addition/removal of peaks was performed if needed [13 ± 2 (mean ± SEM) manual corrections of individual heartbeats on average].

The accuracy of the heartbeat detection procedure from ICA-EEG was subsequently validated in a dataset of 13 participants (8 patients, included in the 68 patients analyzed here, and 5 additional healthy participants) where a regular EKG was also recorded. The validation consisted of a Pearson correlation of interbeat interval time series and power spectrum between 0 and 0.4 Hz, and the percentage error of the power in the three frequency bands typically used to study heart rate variability (HRV; 0.03–0.04, 0.04–0.15, and 0.15–0.4 Hz; Task Force of the European Society of Cardiology the North American Society of Pacing, 1996).

Heartbeat-evoked responses. The HER corresponds to brain activity evoked by each heartbeat and can be analyzed by averaging EEG data time locked to heartbeats (Schandry et al., 1986). The HER was computed after the rejection of cardiac artifacts with independent component analysis, bad channel interpolation, and rereferencing to a common average. Epochs of preprocessed EEG data were defined from each R peak to 500 ms after. Epochs with an amplitude >300 μV on any channel, or where the next or preceding heartbeat occurred at an interval <500 ms, were discarded. Epoched data were smoothed using a 30 ms time window with an 80% overlap, resulting in 20 time points.

We generated surrogate heartbeats to test whether locking EEG data to real heartbeats, as in the HER analysis, improves classification accuracy compared with analyzing EEG data at random moments. Heartbeats were reallocated at pseudorandom timings with interbeat intervals >500 ms. In each patient, 1000 surrogate heartbeats were generated to compare classification accuracy obtained using random segments of EEG data locked to surrogate heartbeats and the classification accuracy obtained on EEG data locked to physiological heartbeats. Classification based on 500 ms EEG segments locked to surrogate heartbeats was performed using the same rejection criteria and the same classification features as classification based on EEG epochs locked to heartbeats. Note that a number of 500 ms EEG segments necessarily overlaps with HERs, since the interval between heartbeats falls most of the time in the 500–1000 ms range.

Multivariate analysis. We used a machine learning approach of multivariate analysis to distinguish between MCS and UWS patients (Sitt et

al., 2014; Raimondo et al., 2017; Engemann et al., 2018). We followed good practices for machine learning to maximally reduce the biases of prediction models (Woo et al., 2017; Steyerberg et al., 2018), such as exploration in a training set with cross-validation followed by prospective validation of the model in an independent test sample, as well as chance-level estimation to take into account the influence of an unbalanced number of UWS and MCS patients (Pal, 2005; Verikas et al., 2011).

We first considered a group of 38 patients (training set) for exploration purposes, in which we performed cross-validation to build the prediction model. We performed a threefold cross-validation (MCS/UWS in each fold: 11/2, 10/3, 10/2) without hyperparameter optimization. Its generalization ability was tested in a new, independent set of 30 patients (validation set). Participants were pseudorandomly assigned to the training set (31 MCS and 7 UWS) and the validation set (24 MCS and 6 UWS) to obtain similar proportions of MCS and UWS in both sets by author J.A. The authors performing the prospective validation (D.C.-R. and C.T.-B.) were blind to patients' diagnoses in the validation set.

We used a random forest (RF) classifier, as implemented at https://code.google.com/archive/p/randomforest-matlab/ (Breiman, 2001), with 1000 trees and a number of features at each node equal to the square root of the total amount of features available, and all other parameters set to default. Compared with other classification approaches, such as support vector machines, RF performs better with noisy and high-dimensional data, limits overfitting, and adapts better to unbalanced datasets (Breiman, 2001; Pal, 2005; Verikas et al., 2011). We nevertheless verified that validation accuracies were larger than chance using a permutation test. We estimated chance-level accuracy by computing 1000 classifications where the labels UWS and MCS were randomly assigned, while maintaining the original number of labels in each category as well as the original number of patients in the training and validation sets (Ojala and Garriga, 2010; Combrisson and Jerbi, 2015). We then compared the distribution of chance-level accuracy with the empirical accuracy and derived the corresponding Monte Carlo p value.

An RF classifier is based on a large number of decision trees that choose their splitting features from a bootstrap-sampled subset of features. As a result, one can estimate the relevance of each input feature for classification, using the "Gini impurity index" (Breiman, 2001; Strobl et al., 2008). Additionally, we defined the consciousness score as the proportion of trees that predicted MCS diagnosis. A patient with a consciousness score >0.5 was classified as MCS. If the consciousness score was <0.5, the patient was classified as UWS. Consciousness scores close to 0.5 indicate a more uncertain classification, and consciousness scores tending to 1 or 0 indicate that all decision trees reach the same conclusion (MCS or UWS, respectively). The consciousness score can be viewed as the classifier confidence about the decision.

PET data and correlation with consciousness scores. PET data were preprocessed and analyzed to obtain the PET diagnosis according to the study by Stender et al. (2014). In short, we used Statistical Parametric Mapping (SPM) to contrast the glucose metabolism of each patient with the glucose metabolism of a group of 34 healthy control subjects without known neurologic or psychological illness. The PET-based diagnosis was made by evaluating the relative preservation of regional metabolism, independently from the CRS-R-based diagnosis. In case of complete bilateral hypometabolism of the frontoparietal network cortex, UWS was diagnosed the patient, while partial preservation of the frontoparietal network corresponded to a diagnosis of MCS (Stender et al., 2014).

For further PET analysis, 19 patients were excluded because of the presence of large lesions covering more than two-thirds of the hemisphere, compromising the reliability of anatomic normalization, as proposed by Di Perri et al. (2016). A total of 49 patients was thus included in the correlation between cerebral glucose uptake and consciousness score based on HERs. We used SPM 12 (https://www.fil.ion.ucl.ac.uk/spm/), a toolbox developed for MATLAB (2017a) to identify brain regions in which glucose metabolism correlated with EKG/EEG-based classification. Separate full factorial designs modeled the effect of the PET-based diagnosis (UWS or MCS) and the consciousness score of classifiers (HER or HRV) on cerebral glucose uptake. Proportional scaling was performed to identify regions that showed a relative increase in glucose metabolism with any regressor. T-contrasts were specified for the main effect of the HER/HRV regressors, and for the interaction of the HER/HRV regressor and diagnosis. Results were considered significant at familywise error (FWE)-corrected $p < 0.05$.

HRV. We used standard measurements of HRV as described in the study by the Task Force of the European Society of Cardiology the North American Society of Pacing (1996), in both the time and frequency domains. Standard time domain features included the mean interbeat interval, the SD of the beat-to-beat intervals, and the square root of the mean squared differences of successive intervals. To estimate power spectral density, we used the Burg periodogram of order 7, a method based on autoregressive spectral estimation, which uses parametric methods to model the data (Thayer et al., 1996). Standard frequency domain features for short-term recordings (5 min) are defined by the power distribution in the following three frequency bands: very low frequency, between 0 and 0.04 Hz; low frequency, between 0.04 and 0.15 Hz; and high-frequency, between 0.15 and 0.4 Hz.

Statistical analysis. Statistical comparisons were based on Mann–Whitney tests, paired t tests, χ^2 tests, or Pearson correlations, as specified in the Results. Classification accuracy significance was assessed with a cumulative binomial distribution and/or Monte Carlo permutation tests. Monte Carlo p values (p_{mc}) were computed as the proportion of the number of classifications (of the 1000 permutations) in which a higher accuracy was reached in permuted data than in empirical data. How permutation tests were designed is specified in the corresponding sections of the Material and Methods. Because computing Monte Carlo p values is computationally intensive, this method could not be used on each of the 1000 draws of random EEG segments. We thus also computed binomial p values (p_{bin}), considering the number of patients as the number of observations and tested the accuracy significance considering a probability of 0.5 (i.e., 1/number of possible diagnosis). To assess binomial significance of the classification on random EEG segments, binomial p values were computed as the proportion of the number of classifications (of the 1000 draws of random EEG segments) in which p_{bin} significance was not reached at $\alpha = 0.05$.

Bayes factors (BFs) were computed to estimate evidence for the null hypothesis H_0 using the CRAN package BayesFactor version 0.9.12–4.2 for R as implemented in https://richarddmorey.github.io/BayesFactor/ (Rouder et al., 2009); with default prior r scale $\sqrt{2}/2$ and substantial evidence for H_0 if BF < 0.3125 (Kass and Raftery, 1995). The statistical analysis of PET data is described in the PET data section.

Data availability.
The data supporting this article, which include sensitive health-related information, are available on reasonable request to the Liège Coma Science Group coma@uliege.be. Codes are publicly available at https://github.com/diegocandiar/brain_heart_doc/.

Results

Heartbeat detection validation
We first extracted the electrocardiogram from ICA-EKG (Raimondo et al., 2017). To validate this approach (Fig. 1), we compared ICA-EKG with real EKG in 13 subjects (8 patients and 5 additional healthy control subjects) where EKG was recorded. Heartbeats were detected independently in EKG and ICA-EKG. The interbeat interval time series obtained from real EKG and ICA-EKG showed a correlation >0.99 in all 13 subjects (Pearson correlation coefficient range, 0.9928–0.9999). Delays of one or two samples between R peaks detected in the real EKG and ICA-EKG could be occasionally observed (Fig. 1C). These minor discrepancies had very limited impact on the spectral analysis of HRV (Pearson correlation coefficient between spectral densities estimated from real EKG and ICA-EKG, range 0.9970-1; the relative difference between real EKG and ICA-EKG in HRV power in very low-, low- and high-frequency ranges is <5% in all participants).
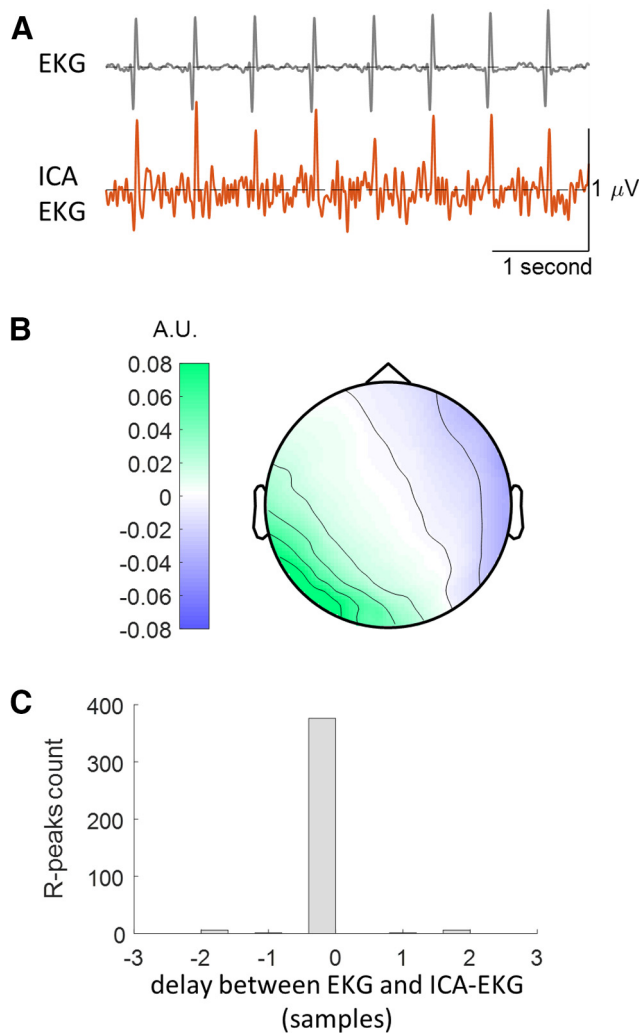
A

B

C

Figure 1. Extraction of the electrocardiogram from EEG data: an example in one patient where both EEG and EKG were acquired. **A**, Real electrocardiogram acquired from chest electrodes (EKG, top) and electrocardiogram extracted from EEG data (ICA-EKG, bottom). **B**, Typical topography of the cardiac-related ICA component, corresponding to the cardiac artifact in EEG data. **C**, Histogram of delays between R peaks measured in EKG and ICA-EKG. Within the 390 heartbeats recorded in 5 min, most R peaks were perfectly aligned, and only 14 (3.6%) R peaks showed a delay of one or two samples (2–4 ms). A.U.: arbitrary units.

Decoding residual consciousness associated with preserved glucose metabolism using heartbeat-evoked responses: exploration in the training sample

We then tested whether HER amplitude and variance could distinguish between UWS and MCS patients in the training sample ($n = 38$). To determine the latencies at which HERs are informative, we computed an independent classifier based on HERs averaged using 200-ms-long sliding time windows and performed a threefold cross-validation to estimate classifier performance in each time window. As shown in Figure 2A, accuracy peaked at 81.62% in the time window between 200 and 400 ms after R peak. To verify that classification results were not driven by cardiac electrical activity (Fig. 2B), we computed the mean ICA-EKG amplitude in the 200–400 ms time interval and found that it does not reliably distinguish between MCS [17.72 ± 15.89 (mean ± SEM)] and UWS patients (−3.55 ± 9.11; Mann–Whitney U test, rank sum = 622; z value = 0.64, p = 0.52; BF = 0.44, inconclusive evidence for H_0). In addition, we performed

RF classification using all the EKG samples of the 200–400 ms time window, and found that accuracy (75.06 ± 4.51%) was much lower than with EEG (81.62%). Because visual inspection suggests a difference in EKG around the R peak, we repeated the same analysis for the time window −100 to +100 ms, and again found a lower accuracy (78.32 ± 3.31%) than in EEG. Moreover, the topography of HERs in the 200–400 ms time window (Fig. 2C) was quite different from the typical cardiac artifact distribution (Fig. 1B; Dirlich et al., 1997).

Having determined the time window of interest, we proceeded to test whether HER amplitude and variance at each time sample between 200 and 400 ms and at each channel could discriminate between UWS and MCS patients using threefold cross-validation. The RF classifier had an accuracy of 81.62% in the training sample. The most relevant channels for RF classification (Gini index averaged across amplitude and variance and across time stamps) were located over right temporal and central regions (Fig. 2D). A sustained difference in HERs between UWS and MCS patients could be observed at those locations (Fig. 2E). Classification relied more on HER variance than HER average (paired-sample t test between Gini impurity indices, $t = −3.7411$, df = 63, $p = 0.0004$). The analysis of the training sample thus indicates that HERs carry relevant information to detect residual signs of consciousness.

We then tested whether patients' classification using HERs outperforms classification based on EEG segments of the same duration, but not locked to heartbeats. Training classifiers with EEG segments not locked to heartbeats led to a threefold cross-validation classification accuracy of 79.08 ± 0.7% in the training sample (average across 1000 classifiers trained on different random selection of EEG segments). Classification accuracy based on random EEG segments is significantly lower than when EEG is locked to heartbeats (81.62%; Monte Carlo test, $p_{mc} < 0.001$; Table 2). Indeed, none of the 1000 classifications performed on random EEG segments had a higher classification accuracy than the classification on HERs, indicating that classification based on HERs is significantly more accurate than classification based on random EEG segments with a $p_{mc} < 0.001$. Brain responses to heartbeats thus convey specific additional information on residual consciousness, compared with generic EEG features.

Decoding residual consciousness using heartbeat-evoked responses: blind prospective validation in a new sample

Following classification good practices (Woo et al., 2017; Steyerberg et al., 2018), we tested whether such results would generalize to a new sample of 30 participants (blind prospective validation). We trained a classifier using all the folds of the training sample ($n = 38$) and confirmed that the model classifies all patients in the training set with a 100% accuracy before assessing the predictions of this classifier in the validation sample. The classifier reached an accuracy of 86.67% (binomial test, $p_{bin} < 0.001$), a sensitivity of 95.8%, and a specificity of 50% in the validation sample.

We ran two additional control analyses. First, because our sample is unbalanced with more MCS ($n = 31$) than UWS ($n = 7$) patients, we verified that results were not because of chance. To estimate chance-level classifier accuracy because of sample imbalance, we computed 1000 classifiers on the same data after randomly reassigning diagnoses across patients, thus maintaining the MCS/UWS imbalance. Chance-level accuracy was on average 77.05 ± 3.98%, almost 10 points lower than the accuracy of the classifier trained on real data. Only one random permutation of 1000 exceeded the accuracy of the classifier trained on the real data, showing that the hypothesis that the 86.67% accuracy of the classifier trained on real data are because of chance can be
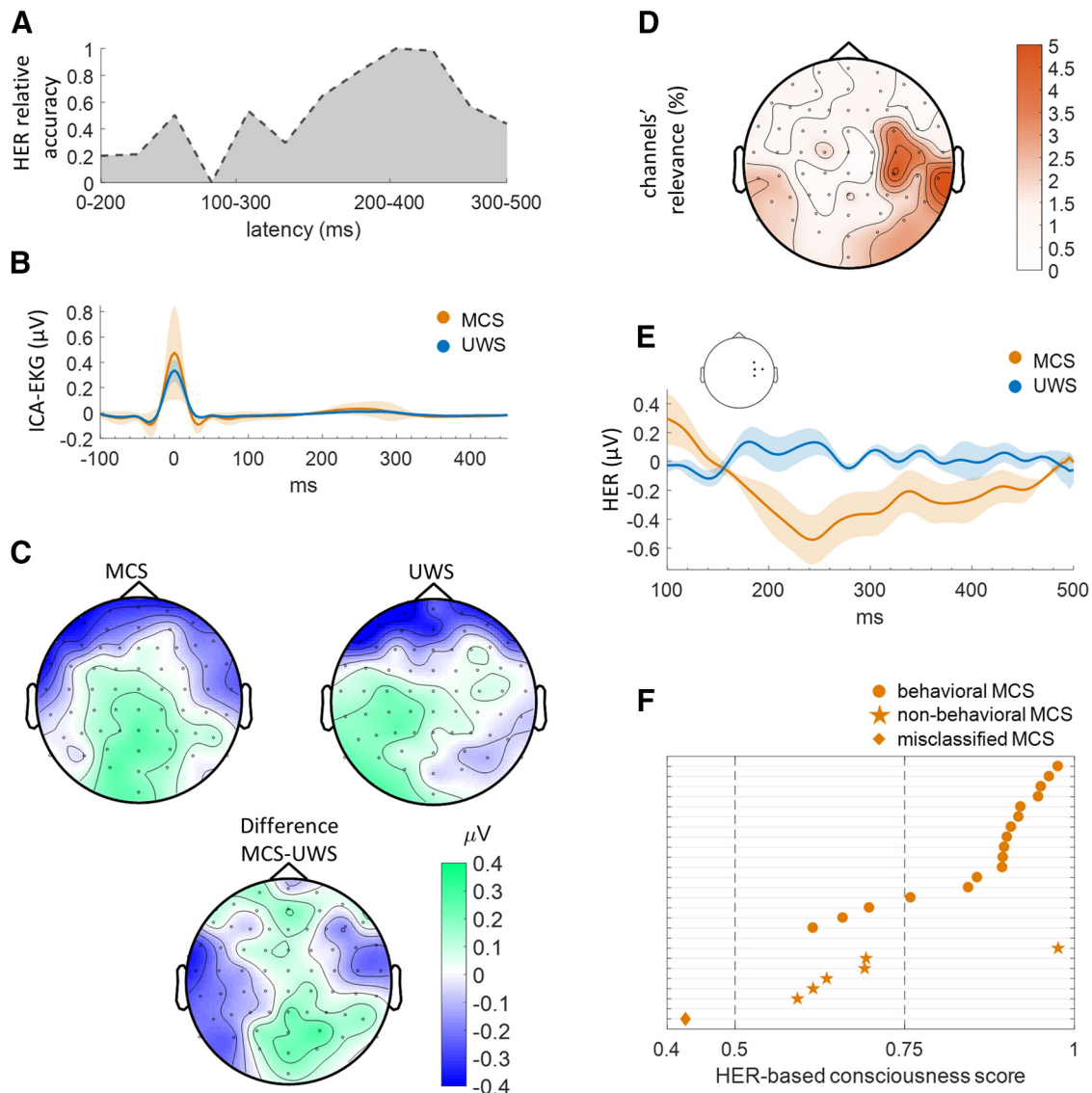
Figure 2. Classification of PET-based diagnosis of consciousness based on heartbeat-evoked responses. ***A***, Classification accuracy in sliding 200-ms-long time windows in a threefold cross-val-idation with HER amplitude and variance at each channel as features, using the consciousness diagnosis obtained from brain glucose metabolism measure with FDG-PET, in the training sample. Accuracy peaks in the 200–400 ms window. Accuracies have been normalized (posterior minimum-maximum normalization to unitary variance), one corresponding to the best accuracy across all time windows. ***B***, ICA-EKG in MCS and UWS patients does not differ between 200 and 400 ms. ***C***, HER topographies averaged between 200 and 400 ms, for MCS patients, UWS patients, and between-group difference in the training sample. The topographies markedly differ from the cardiac artifact (Fig. 1*B*) and indicate the neural origin of HERs. ***D***, Topography of channel relevance in the training sample, based on both amplitude and variance of HERs, showing a larger contribution of left and right occipitotemporal electro-des as well as of right central and temporal electrodes. ***E***, Group-averaged HERs in the training sample, averaged across right central channels, showing a sustained difference between 200 and 400 ms. ***F***, HER-based consciousness scores in the independent validation sample, showing low HER-based consciousness scores, are more likely to correspond to nonbehavioral MCS than to behavioral MCS.

rejected with $p_{mc} = 0.001$. Second, we applied the same proce-dure to EEG segments not locked to heartbeats and found a mean classification accuracy in the validation sample of $80.84 \pm 4.09\%$ (binomial test over 1000 permutations, $p_{bin} < 0.001$; i.e., 6 points below the classification of the classifier based on HERs, a difference that was only marginally significant; com-parison between the distribution of the 1000 classifications on random EEG segments with HER-based classifier, $p_{mc} = 0.064$). Altogether, the classification results in the validation sample (Table 2) show that HERs provide reliable information about re-sidual signs of consciousness in MCS patients that can be gener-alized to a new dataset and confirm that HERs convey specific consciousness-related information beyond what can be extracted from EEG data not locked to heartbeats.

Nonbehavioral MCS patients have smaller HER-based consciousness scores

So far, we have considered the diagnosis of consciousness based on brain glucose metabolism (PET-based diagnosis), because this diagnosis is independent from overt behavior. However, clinical diagnosis is most often based on a behavioral index, here based on the best CRS-R subscore, but is not always consistent with the PET-based diagnosis (Gosseries et al., 2014; Stender et al., 2014; Schiff, 2015). In the current dataset, the diagnosis of UWS based on PET data was consistent with the CRS-R diagno-sis in all UWS patients. However, patients with a PET-based di-agnosis of MCS could be split into two categories: behavioral MCS ($n = 18$), i.e. patients considered as MCS based on both brain metabolism and best CRS-R diagnosis, and non-behavioral

Table 2. Summary of main results

		Threefold cross-validation accuracy, training sample	Monte-Carlo comparison between HER and random EEG segments	Accuracy in validation sample (test against chance)	Comparison between HER and random EEG segments
PET-based consciousness diagnosis	HER 200–400 ms	81.62%	$p_{mc} < 0.001$	86.67% ($p_{bin} < 0.001$, $p_{mc} = 0.001$)	$p_{mc} = 0.064$
	Random EEG segments (mean $\pm$ SD across 1000 permutations)	79.08 $\pm$ 0.7%		80.84 $\pm$ 4.09% ($p_{bin} < 0.001$)	
CRS-R-based consciousness diagnosis	HER 156-356 ms	79.06%	$p_{mc} = 0.038$	76.67% ($p_{bin} < 0.001$, $p_{mc} = 0.004$)	$p_{mc} = 0.041$
	Random EEG segments (mean $\pm$ SD across 1000 permutations)	72.95 $\pm$ 4.49%		66.42 $\pm$ 7.13% ($p_{bin} = 0.272$)	

Classifications based on HERs consistently outperform classifications based on random EEG segments. Classifications using PET-based diagnosis consistently outperform classifications using CRS-R-based diagnosis.

MCS (or MCS*, $n = 6$), i.e. patients showing only reflex-like behavior as measured with CRS-R, yet with a brain metabolism suggesting a capacity for consciousness (Gosseries et al., 2014).

For each patient identified as being in an MCS based on PET diagnosis, we computed a HER-based consciousness score, defined as the proportion of decision trees of the HER-based classifier predicting MCS diagnosis (Fig. 2F). This score can be viewed as the confidence of the classifier in the diagnosis, with four ranges (0–0.25, UWS with high certainty; 0.25–0.5, UWS with low certainty; 0.5–0.75, MCS with low certainty; and 0.75–0.1, MCS with high certainty). Patients with consciousness scores indicating MCS with low certainty were significantly more likely to be nonbehavioral MCS patients: the proportion of nonbehavioral MCS patients was significantly larger in low-certainty MCS patients (55%; 5 of 9) than in high-certainty MCS patients (6.6%; 1 of 15; χ^2 test, χ^2 statistic = 7.17, $p = 0.007$).

HER-based consciousness scores correlate with PET metabolism in right occipitotemporal and lateral temporal regions

We next tested whether consciousness-related information conveyed by HERs correlated with glucose metabolism in specific brain regions (according to AAL Atlas, Tzourio-Mazoyer et al., 2002), in an exploratory analysis. Across both the training and test sets, we identified 49 patients (39 MCS, 10 UWS; based on FDG-PET) whose brain anatomy allowed anatomic normalization, trained a classifier on HERs in those patients, and correlated the resulting HER-based consciousness scores with glucose metabolism. A positive correlation between glucose metabolism and HER-based consciousness scores was found in the right temporal lobe in the 39 MCS patients (Table 3, Fig. 3). The largest cluster extended along the right ventral occipitotemporal regions. Neurosynth (Yarkoni et al., 2011) reveals that this region is functionally connected mostly to its homologous region in the left hemisphere, and that it is strongly associated with the terms "face," "face recognition," and "object recognition," as expected from the known functional organization of the ventral visual system (Mishkin et al., 1983; Haxby et al., 1991; Kanwisher et al., 1997). The second region was located in the anterior part of the right superior temporal sulcus. This region has a much richer pattern of functional connectivity, as revealed by Neurosynth, being connected to the core components of the default network (i.e., ventromedial prefrontal cortex, posterior cingulate cortex, right inferior parietal lobule, as well as the right amygdalo-hippo-campal region and the homologous region in in the left hemisphere). The lateral temporal region is loosely associated with a larger number of terms, related to social interactions ("social cognitive," "theory of mind," "sentence comprehension") but

Table 3. Significant brain regions that correlate with consciousness score in MCS patients

Cluster	Brain regions	Voxels, n	Area, mm^3	t Value peak	x	y	z
1	Temporal inf R	338	2704	5.494091	48	−48	−22
	Fusiform R	165	1320	5.415044	46	−50	−20
	Occipital inf R	149	1192	5.088109	48	−62	−14
	Lingual R	13	104	4.532592	24	−90	−10
2	Temporal mid R	86	688	4.845305	48	0	−22
	Temporal inf R	44	352	4.775336	44	−10	−36
	Fusiform R	18	144	4.723663	40	−8	−36
	Temporal pole mid R	3	24	4.513527	46	6	−24
	Temporal pole sup R	1	8	4.533496	46	2	−20
3	Temporal sup R	5	40	4.482989	64	−22	0

Anatomical labels according to AAL Atlas (Tzourio-Mazoyer et al., 2002). R, Right; inf, inferior; mid, middle; sup, superior. x,y,z MNI coordinates are provided.

also to internal, self-related cognition ("default network," "auto-biographical"). No significant correlation could be found between HER-based consciousness score and PET metabolism in the 10 UWS patients.

Using HERs to decode consciousness as diagnosed from CRS-R

In this study, we explore markers of consciousness independent from behavior. However, the measure of consciousness most commonly used in clinical practice is behavioral assessment with the CRS-R. We thus tested whether we could decode consciousness as diagnosed with CRS-R using HERs, using the same procedure as used for decoding consciousness as diagnosed with PET, and compared CRS-R-based classification accuracy to PET-based classification accuracy.

To determine the latencies at which HERs are informative, we computed an independent classifier based on HERs averaged using 200-ms-long sliding time windows and performed a three-fold cross-validation to estimate classifier performance in each time window. The best candidate time window to decode consciousness as diagnosed with CRS-R in the training sample was 156–356 ms (i.e., quite close to the best time window to decode consciousness from PET diagnosis, which was 200–400 ms). We then trained a classifier with HER amplitude and variance at each channel and each time sample of the 156–356 ms time window using threefold cross-validation. The accuracy of classification based on CRS-R diagnosis was 79.06% (binomial test, $p_{bin} < 0.001$), which is somewhat lower than the classification based on PET diagnosis (threefold cross-validation accuracy, 81.62%). HERs did convey a significant advantage to CRS-R-based classification: classifications performed on random EEG segments led to an average accuracy of 72.95 $\pm$ 4.49% (binomial test over 1000
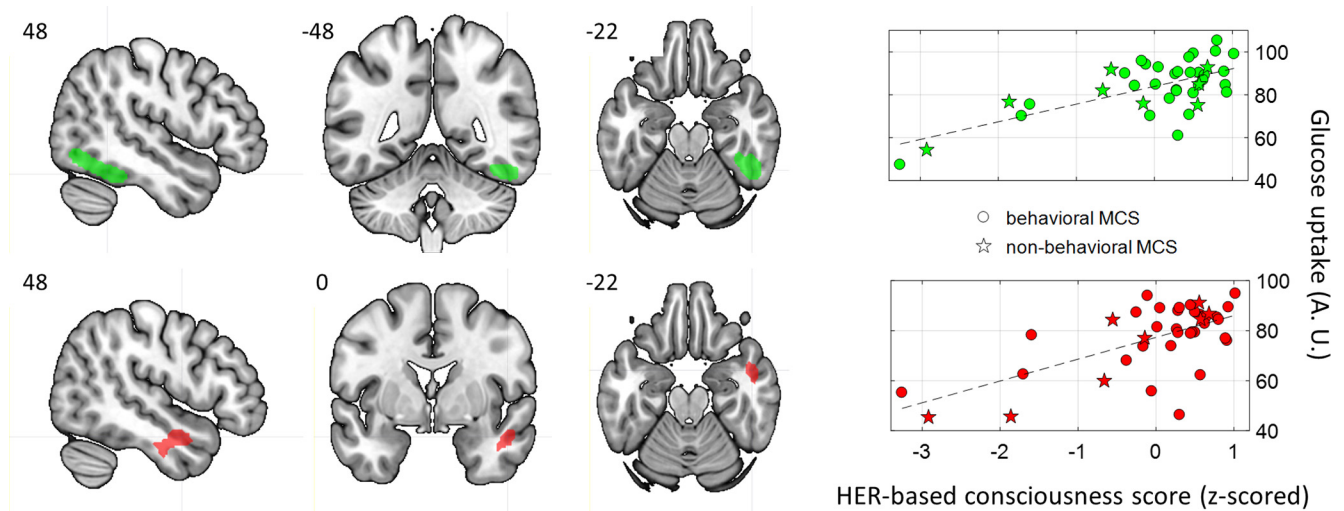
Figure 3. Glucose metabolism correlates of HER-based consciousness scores in MCS patients ($n = 39$). Top, Right ventral occipitotemporal regions (MNI coordinates: 48, −48, −22; FWE corrected, p value cluster = 0.002). Bottom, Right anterior superior temporal sulcus (MNI coordinates: 48, 0, −22; FWE corrected, p value cluster = 0.012). A.U.: arbitrary units.

permutations, $p_{bin} = 0.012$), whereas HER-based classification accuracy was 79.06% (comparison between the accuracies distribution of the 1000 classifications on random EEG segments and the HER-based classifier accuracy, $p_{mc} = 0.038$).

We then trained a CRS-R-based classifier on all the folds of the training sample ($n = 38$) and tested the performance of this classifier in the validation set ($n = 30$; blind prospective cross-validation). The classification performed over CRS-R diagnosis reached an accuracy of 76.67%, which is significantly above chance (chance accuracy obtained by randomly shuffling diagnosis labels, $59.53 \pm 5.34\%$; 4 of 1000 permutations outperformed classification on real diagnosis, $p_{mc} = 0.004$). HERs did convey a significant advantage to CRS-R-based classification, as compared to EEG segments not locked to heartbeats (EEG segments, mean classification accuracy $66,42 \pm 7.13\%$, binomial test over 1000 permutations, $p_{bin} = 0.272$; HER-based classification accuracy, 76.67%, binomial test, $p_{bin} < 0.001$, Monte Carlo test, $p_{mc} = 0.041$). However, the blind prospective classification based on CRS-R diagnosis remained 10 points lower than the accuracy of the classifier based on PET diagnosis, which was 86.67% (Table 2). Finally, when the classification used CRS-R diagnosis, HER consciousness scores did not correlate with brain glucose metabolism in any region. HER classification using the CRS-R diagnosis of consciousness thus partly reproduces the results obtained with HER classification using the PET diagnosis of consciousness, showing a better accuracy of HERs than random EEG segments. However, the generalization accuracy of the CRS-R-based HER classifier was much lower than the generalization accuracy of the PET-based HER classifier. This suggests an underlying better consistency between two brain measures of consciousness (PET glucose metabolism and HERs) than between a behavioral measure of consciousness (CRS-R) and a neural measure (HER). Of note, in the present study, the difference between CRS-R diagnosis and PET diagnosis is exclusively found in MCS* patients, where PET indicates minimal consciousness while CRS-R indicates unconsciousness. All five behavioral assessments using CRS-R, including the one performed at the time of EEG-PET data acquisition, indicated unconsciousness in all MCS* patients with 100% consistency over time. The difference between PET-based diagnosis and CRS-R diagnosis thus seems to correspond to a reliable difference between the methods of assessments rather than to fluctuations in behavior.

No reliable decoding of residual consciousness using heart rate variability

Our results show that HERs, reflecting how the brain responds to ascending signal at each heartbeat, could accurately distinguish MCS from UWS patients, especially when using PET-based consciousness diagnosis, which is independent from overt behavioral responses. We further tested whether heart rate variability, which is strongly constrained by descending signals from brain to heart, can distinguish between MCS and UWS during the resting state. We first investigated, using a standard univariate approach (Mann–Whitney U tests between MCS and UWS), whether routinely used measures of HRV would differ between MCS and UWS patients in the training set. None of the classical measures (Task Force of the European Society of Cardiology the North American Society of Pacing, 1996) we computed could reliably distinguish between MCS and UWS patients (Table 4).

Although neither the low- nor high-frequency power of HRV could distinguish between MCS and UWS, the HRV power spectrum density showed qualitative differences (Fig. 4A), suggesting that the full power spectrum is a good candidate for multivariate analysis. Using HRV frequency power at 13 different frequencies as features, we obtained a threefold cross-validation accuracy of 79.06% in the training sample. Two frequency ranges were particularly relevant for classification (Fig. 4B), ~0.1–0.2 Hz and ~0.3–0.4 Hz, which differ slightly from the classical low-frequency (0.04–0.15 Hz) and high-frequency (0.15–0.4 Hz) HRV ranges (Task Force of the European Society of Cardiology the North American Society of Pacing, 1996). We then trained a classifier using all folds from the training set, reaching a 100% accuracy. We tested this classifier in the independent validation sample of 30 patients, which resulted in an accuracy of 76.67%. HRV validation accuracy was not significantly different from chance accuracy ($p_{mc} = 0.382$) and was 10 points lower than HER validation accuracy (86.67%).

The classification based on HER and the classification based on HRV generated different predictions, and misclassified patients with one or the other method were different (Fig. 4C). Consciousness scores obtained from the HRV-based classifier

Table 4. Heart rate variability univariate analysis

Heart rate variability feature	MCS (mean ± SD)	UWS (mean ± SD)	Mann–Whitney U test p value uncorrected for multiple comparisons	Rank sum	z Value
Mean interbeat intervals (ms)	892 ± 194	817 ± 134	0.3661	629	0.9037
SD of interbeat intervals (ms)	47 ± 24	34 ± 23	0.1525	643	1.4309
Root mean square of successive differences (ms)	37 ± 29	19 ± 13	0.0768	652	1.7698
Very low-frequency power (ms^2)	$1.64 \pm 4.04\ 10^7$	$3.83 \pm 4.88\ 10^7$	0.4743	585	−0.7155
Low-frequency power (ms^2)	468 ± 571	207 ± 276	0.1752	641	1.3556
High-frequency power (ms^2)	637 ± 840	180 ± 189	0.1320	645	1.5062
Low-/high frequency ratio	1.68 ± 2.09	1.54 ± 2.11	0.8213	611	0.2259

did not correlate with the consciousness scores obtained from the HER-based classifier (Pearson correlation $r = -0.1512$, $p = 0.4251$, BF = 0.5241; inconclusive evidence for H_0). These results suggest that HER-based and HRV-based classifications might be complementary. We thus tried to combine predictions based on HER and HRV by applying the following rule: a patient is classified MCS if both the HER-based and HRV-based consciousness scores are >0.5, otherwise the patient is classified as UWS. This procedure led to an accuracy of 83.33% (binomial test, $p_{bin} <$ 0.001) in the validation sample [i.e., a lower accuracy than with HER-based classification only (86.67%)]. However, combining HER- and HRV-based classifications led to a better balance between sensitivity and specificity, compared with HER only.

Discussion

Because ascending signals from heart to brain have been associated with different aspects of consciousness in healthy participants (Park et al., 2014, 2016; Babo-Rebelo et al., 2016a,b, 2019; Sel et al., 2017), we hypothesized that neural responses to heartbeats would differ in MCS compared with UWS patients. We found that heartbeat-evoked responses could accurately distinguish MCS and UWS patients in an independent validation sample with an accuracy of 87%, (sensitivity, 96%; specificity, 50%), when the consciousness diagnosis was based on glucose uptake as measured with PET (i.e., a diagnosis independent from behavioral output). Using HERs as features systematically led to classifier accuracies that were larger than when using on random EEG segments or heart rate variability as features, showing that how the brain responds to heartbeats provides additional information on consciousness, compared with generic ongoing EEG activity or to heart rate. HER-based classification offered not only a dichotomous classification between UWS and MCS patients but also a more graded and individualized consciousness score that captured some of the complexity of the clinical diagnosis, with low consciousness scores being much more frequent in nonbehavioral MCS. HER-based consciousness scores correlated with glucose metabolism in the default mode network node located in the right superior temporal sulcus, as well as with the right ventral occipitotemporal cortex. HERs predicted consciousness better when consciousness was inferred from glucose metabolism than when consciousness was inferred from behavior using CRS-R diagnosis. Our results indicate that the transient brain responses elicited at each heartbeat convey relevant information on residual consciousness that does not necessarily translate into behavior, in patients with chronic disorders of consciousness.

HERs improve the detection of residual consciousness
HERs correspond to brain responses to ascending cardiac inputs at each heartbeat. So far, cardiac-related indexes of consciousness have been obtained from HRV, which characterizes descending control of the brain on cardiac rhythm. HRV distinguishes

between UWS and MCS patients receiving nociceptive stimulation (Leo et al., 2016; Tobaldini et al., 2018; Riganello et al., 2018a); auditory stimulation (Raimondo et al., 2017); or at rest and under sedation (Riganello et al., 2018b). Here, we show that HERs are more efficient to distinguish between UWS and MCS patients in the resting, awake state than HRV. Several lines of evidence suggest that the difference in HERs between MCS and UWS is of cerebral origin, rather than cardiac electrical activity detected at the sensor level. First, we could not find any EKG amplitude difference between MCS and UWS patients, indicating that the HER effect is not directly driven by cardiac electrical activity. Second, the most relevant channels to distinguish between MCS and UWS patients were located at right central sites, while the EEG channels most affected by the cardiac artifact display the typical topography over left temporal and right frontal regions (Dirlich et al., 1997). Third, HER and HRV provided nonredundant information on consciousness. Last, HER-based consciousness scores correlated with brain glucose uptake measured with PET in right temporal regions, suggesting that HER-based classification is directly related to brain activity.

A number of studies have successfully used EEG to predict unconsciousness/consciousness, with prospective validation accuracies in the 71–78% range (Engemann et al., 2018). Our own results when using random EEG segments not locked to heartbeats (prospective validation accuracy, 81%) were commensurate with the literature, and confirm that generic EEG features, as captured by random EEG segments not locked to heartbeats, do provide valuable information to detect residual consciousness. However, the classifications we performed on HERs, using both amplitude (Raimondo et al., 2017) and variance from one trial to the next as features, were systematically more accurate than those performed on random EEG segments. HERs thus convey reliable and specific information about residual consciousness in addition to that provided by the generic EEG features captured by random EEG segments.

HERs as an indicator of conscious inner mental life even in the absence of behavior
The hypothesis that motivated this work is that HERs contribute to subjective experience (Park and Tallon-Baudry, 2014; Tallon-Baudry et al., 2018; Azzalini et al., 2019). While the results are in keeping with this hypothesis, alternative interpretations have to be considered.

HERs might be a marker of an overall brain state fostering consciousness, such as arousal. However, an overall brain state should also be reflected in neural activity not locked to heartbeats, whereas we found a systematic advantage to classifications based on HERs over classifications based on random EEG segments. In addition to, the correlations between glucose uptake and HER-based consciousness scores did not occur in brain regions associated with arousal, such as the saliency network. Last,
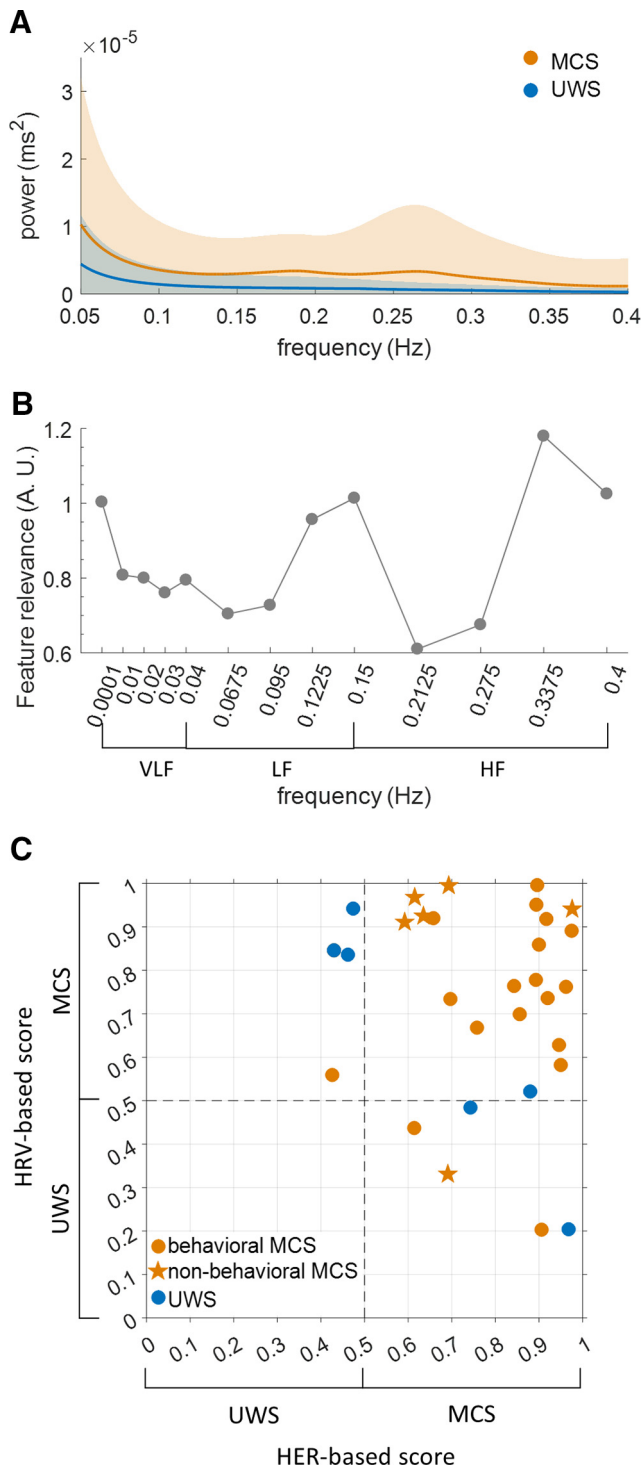
Figure 4. Classifications based on the spectral analysis of heart rate variability. ***A***, HRV power spectrum density of MCS and UWS patients in the training sample. ***B***, Relevance of each frequency (Gini impurity index) to the HRV-based classifier in the training sample, with most relevant frequencies at the border between low-frequency (LF) HRV and high-frequency (HF) HRV and at the upper limit of HF HRV. The contribution of very low frequencies (VLFs) appears limited. ***C***, Consciousness scores obtained from the classifier trained on HRV plotted against consciousness scores obtained from the classifier trained on HERs, in the independent validation sample ($n = 30$).

in healthy participants, consciousness-related modulations of HERs were not accompanied by changes in arousal (Park et al., 2014; Babo-Rebelo et al., 2016a, 2019). The difference between classifications based on random EEG segments and segments

aligned to cardiac events is thus likely to be attributed to a change in EEG amplitude and/or variance occurring specifically after heartbeats (i.e., the definition of a heartbeat-evoked response).

If HERs do not reflect a global brain state, then what do they reflect? HERs might convey consciousness-related information about how the brain responds to an internal stimulus, much as responses to exteroceptive stimuli (Cruse et al., 2011; Sitt et al., 2014) or artificial stimuli such as transcranial magnetic pulses (Casali et al., 2013; Casarotto et al., 2016) are informative about consciousness state. However, we did not find any link between HER-based consciousness scores and glucose uptake in interoceptive regions such as primary somatosensory cortex (Kern et al., 2013) or insula (Park et al., 2018). The present results relating HERs to residual consciousness in patients appear more congruent with the covariation between HERs and perceptual, bodily, and self-consciousness (Park et al., 2014, 2016; Babo-Rebelo et al., 2016a,b, 2019; Sel et al., 2017; Al et al., 2020) observed in healthy participants.

We could link HER-based classification results to glucose metabolism in two regions, which are very different from the frontoparietal regions used to determine the diagnosis of consciousness based on glucose metabolism. The right occipito-temporal cluster corresponds to areas involved in visual shape analysis, while the right anterior superior temporal sulcus is known for its role for in spontaneous, potentially self-related, cognition (Andrews-Hanna et al., 2010), as well as in self-recognition and theory of mind (van Veluw and Chance, 2014). The right lateralization of the brain regions whose glucose metabolism correlates with HER-based classification scores, as well as of the electrodes contributing to the HER-based classification, is reminiscent of nonverbal consciousness in the right hemisphere of split-brain patients (Sperry, 1984).

Consciousness is defined by the existence of subjective experience and inner mental life, a feature that does not necessarily translate into overt behavior. HERs appear here as a valid indicator of inner mental life, since HER-based classification successfully detects residual consciousness even during resting state without behavioral reports, and even in nonbehavioral MCS patients, who never showed any behavioral sign of consciousness. HERs might thus help to specify the gray zone of consciousness (i.e., the fleeting conscious feelings that might not be cognitively accessed or translate into behavioral outputs). This interpretation is in keeping with the fact the HER-based classification is in better agreement with the consciousness diagnosis based on brain metabolism than with the consciousness diagnosis based on behavior. It is worth noting that this better agreement does not reflect a mere correlation between two different measures of brain activity, independently of the notion of consciousness, since the link between HERs and glucose metabolism is mediated by the consciousness diagnosis on which the HER classifier is trained. Because measuring consciousness in the absence of overt behavior is challenging, cross-validating measures of consciousness is an important step to detect consciousness at the cerebral level, rather than at the behavioral level, be it at bedside (Bodart et al., 2017) or in healthy participants (Tsuchiya et al., 2015; Bayne et al., 2017).

Potential clinical relevance

Observations that heartbeat-evoked responses are linked to consciousness in healthy adults (Park et al., 2014, 2016; Babo-Rebelo et al., 2016a,b, 2019; Sel et al., 2017) could lead to a new sensitive tool to identify residual consciousness and establish fine-grained stratification in patients with disorders of consciousness, with

only 5 min of resting-state EEG data that can easily be acquired at bedside, which could prove particularly valuable when PET, fMRI, or transcranial magnetic stimulation-EEG are not available or cannot be used for safety reasons. Note that recording an EKG together with EEG would markedly improve the procedure, since the extraction of EKG from EEG using ICA is not always possible. Because the experimental situation does not require the active involvement of the patient beyond being awake, the patient's specific sensory impairments or cognitive deficits should have a limited impact on HER-based classification. Still, the clinical relevance of neural responses to heartbeats remains to be validated in a larger multisite cohort, with more UWS patients and patients with long-term outcomes. When assessing consciousness along multiple dimensions (Sitt et al., 2014; Bayne et al., 2017; Sergent et al., 2017; Song et al., 2018), neural responses to heartbeats could contribute to the evaluation of more experiential aspects of consciousness, potentially corresponding to fleeting conscious feelings not accompanied by behavioral signs of consciousness and not detected by standard clinical assessment based on CRS diagnosis, rather than fully developed intentional communication that translates into behavior.

Conclusion

HERs convey specific information on residual consciousness in patients, compared with EEG not locked to heartbeats. This result lends support to the hypothesis that HERs play a role in generating conscious experience (Park and Tallon-Baudry, 2014; Tallon-Baudry et al., 2018; Azzalini et al., 2019) and complement a number of experimental results in healthy participants pointing in the same direction (for review, see Azzalini et al., 2019). We further showed that HERs capture the consciousness diagnosis based on brain metabolism during resting state better than the consciousness diagnosis based on behavior. It is thus possible to conceptualize and experimentally test consciousness as an experiential phenomenon, rather than as an intermediate cognitive step between external input and behavioral output.

References

Al E, Iliopoulos F, Forschack N, Nierhaus T, Grund M, Motyka P, Gaebler M, Nikulin VV, Villringer A (2020) Heart–brain interactions shape somatosensory perception and evoked potentials. Proc Natl Acad Sci U S A 117:10575–10584.

Andrews-Hanna JR, Reidler JS, Sepulcre J, Poulin R, Buckner RL (2010) Functional-anatomic fractionation of the brain's default network. Neuron 65:550–562.

Azzalini D, Rebollo I, Tallon-Baudry C (2019) Visceral signals shape brain dynamics and cognition. Trends Cogn Sci 23:488–509.

Babo-Rebelo M, Richter CG, Tallon-Baudry C (2016a) Neural responses to heartbeats in the default network encode the self in spontaneous thoughts. J Neurosci 36:7829–7840.

Babo-Rebelo M, Wolpert N, Adam C, Hasboun D, Tallon-Baudry C (2016b) Is the cardiac monitoring function related to the self in both the default network and right anterior insula? Philos Trans R Soc Lond B Biol Sci 371:20160004.

Babo-Rebelo M, Buot A, Tallon-Baudry C (2019) Neural responses to heartbeats distinguish self from other during imagination. Neuroimage 191:10–20.

Bayne T, Hohwy J, Owen AM (2017) Reforming the taxonomy in disorders of consciousness. Ann Neurol 82:866–872.

Blanke O, Metzinger T (2009) Full-body illusions and minimal phenomenal selfhood. Trends Cogn Sci 13:7–13.

Block N (2005) Two neural correlates of consciousness. Trends Cogn Sci 9:46–52.

Bodart O, Gosseries O, Wannez S, Thibaut A, Annen J, Boly M, Rosanova M, Casali AG, Casarotto S, Tononi G, Massimini M, Laureys S (2017) Measures of metabolism and complexity in the brain of patients with disorders of consciousness. Neuroimage 14:354–362.

Breiman L (2001) Random forests. Mach Learn 45:5–32.

Candia-Rivera D, Catrambone V, Valenza G (2020a) Methodological considerations on EEG electrical reference: A functional brain-heart interplay study. 42nd Annual International Conference of the IEEE Engineering in Medicine & Biology Society (EMBC), 20–24, July, Montreal, QC, Canada.

Candia-Rivera D, Catrambone V, Valenza G (2020b) The role of EEG electrical reference in the assessment of Functional brain-heart interplay: a preliminary study. 11th Conference of the European Study Group on Cardiovascular Oscillations (ESGCO), 15 July, Pisa, Italy.

Casali AG, Gosseries O, Rosanova M, Boly M, Sarasso S, Casali KR, Casarotto S, Bruno M-A, Laureys S, Tononi G, Massimini M (2013) A theoretically based index of consciousness independent of sensory processing and behavior. Sci Transl Med 5:198ra105.

Casarotto S, Comanducci A, Rosanova M, Sarasso S, Fecchio M, Napolitani M, Pigorini A, Casali AG, Trimarchi PD, Boly M, Gosseries O, Bodart O, Curto F, Landi C, Mariotti M, Devalle G, Laureys S, Tononi G, Massimini M (2016) Stratification of unresponsive patients by an independently validated index of brain complexity. Ann Neurol 80:718–729.

Chalmers DJ (1995) Facing up to the problem of consciousness. J Conscious Stud 2:200–219.

Combrisson E, Jerbi K (2015) Exceeding chance level by chance: the caveat of theoretical chance levels in brain signal classification and statistical assessment of decoding accuracy. J Neurosci Methods 250:126–136.

Cruse D, Chennu S, Chatelle C, Bekinschtein TA, Fernández-Espejo D, Pickard JD, Laureys S, Owen AM (2011) Bedside detection of awareness in the vegetative state: a cohort study. Lancet 378:2088–2094.

Di Perri C, Bahri MA, Amico E, Thibaut A, Heine L, Antonopoulos G, Charland-Verville V, Wannez S, Gomez F, Hustinx R, Tshibanda L, Demertzi A, Soddu A, Laureys S (2016) Neural correlates of consciousness in patients who have emerged from a minimally conscious state: a cross-sectional multimodal imaging study. Lancet Neurol 15:830–842.

Dirlich G, Vogl L, Plaschke M, Strian F (1997) Cardiac field effects on the EEG. Electroencephalogr Clin Neurophysiol 102:307–315.

Engemann DA, Raimondo F, King J-R, Rohaut B, Louppe G, Faugeras F, Annen J, Cassol H, Gosseries O, Fernandez-Slezak D, Laureys S, Naccache L, Dehaene S, Sitt JD (2018) Robust EEG-based cross-site and cross-protocol classification of states of consciousness. Brain 141:3179–3192.

Frässle S, Sommer J, Jansen A, Naber M, Einhäuser W (2014) Binocular rivalry: frontal activity relates to introspection and action but not to perception. J Neurosci 34:1738–1747.

Giacino JT, Ashwal S, Childs N, Cranford R, Jennett B, Katz DI, Kelly JP, Rosenberg JH, Whyte J, Zafonte RD, Zasler ND (2002) The minimally conscious state: definition and diagnostic criteria. Neurology 58:349–353.

Giacino JT, Kalmar K, Whyte J (2004) The JFK Coma Recovery Scale-Revised: measurement characteristics and diagnostic utility. Arch Phys Med Rehabil 85:2020–2029.

Giacino JT, Katz DI, Schiff ND, Whyte J, Ashman EJ, Ashwal S, Barbano R, Hammond FM, Laureys S, Ling GSF, Nakase-Richardson R, Seel RT, Yablon S, Getchius TSD, Gronseth GS, Armstrong MJ (2018) Practice guideline update recommendations summary: disorders of consciousness: Report of the Guideline Development, Dissemination, and Implementation Subcommittee of the American Academy of Neurology; the American Congress of Rehabilitation Medicine; and the National Institute on Disability, Independent Living, and Rehabilitation Research. Arch Phys Med Rehabil 99:1699–1709.

Gosseries O, Zasler ND, Laureys S (2014) Recent advances in disorders of consciousness: focus on the diagnosis. Brain Injury 28:1141–1150.

Haxby JV, Grady CL, Horwitz B, Ungerleider LG, Mishkin M, Carson RE, Herscovitch P, Schapiro MB, Rapoport SI (1991) Dissociation of object and spatial visual processing pathways in human extrastriate cortex. Proc Natl Acad Sci U S A 88:1621–1625.

Jung T-P, Humphries C, Lee T-W, Makeig S, McKeown MJ, Iragui V, Sejnowski TJ (1998) Extended ICA removes artifacts from electroencephalographic recordings. In: Advances in neural information processing systems (Jordan MI, Kearns MJ, Solla SA, eds), pp 894–900. Cambridge, MA: MIT.

Kanwisher N, McDermott J, Chun MM (1997) The fusiform face area: a module in human extrastriate cortex specialized for face perception. J Neurosci 17:4302–4311.

Kass RE, Raftery AE (1995) Bayes factors. J Am Stat Assoc 90:773–795.

Kern M, Aertsen A, Schulze-Bonhage A, Ball T (2013) Heart cycle-related effects on event-related potentials, spectral power changes, and connectivity patterns in the human ECoG. Neuroimage 81:178–190.

Kondziella D, Bender A, Diserens K, van Erp W, Estraneo A, Formisano R, Laureys S, Naccache L, Ozturk S, Rohaut B, Sitt JD, Stender J, Tiainen M, Rossetti AO, Gosseries O, Chatelle C (2020) European Academy of Neurology guideline on the diagnosis of coma and other disorders of consciousness. Eur J Neurol 27:741–756.

Laureys S, Owen AM, Schiff ND (2004) Brain function in coma, vegetative state, and related disorders. Lancet Neurol 3:537–546.

Laureys S, Celesia GG, Cohadon F, Lavrijsen J, León-Carrión J, Sannita WG, Sazbon L, Schmutzhard E, von Wild KR, Zeman A, Dolce G (2010) Unresponsive wakefulness syndrome: a new name for the vegetative state or apallic syndrome. BMC Med 8:68.

Leo A, Naro A, Cannavò A, Pisani LR, Bruno R, Salviera C, Bramanti P, Calabrò RS (2016) Could autonomic system assessment be helpful in disorders of consciousness diagnosis? A neurophysiological study. Exp Brain Res 234:2189–2199.

Luu P, Ferree TC (2000) Determination of the geodesic sensor nets' average electrode positions and their 10–10 international equivalents. Eugene, OR: Electrical Geodesics.

Mishkin M, Ungerleider LG, Macko KA (1983) Object vision and spatial vision: two cortical pathways. Trends Neurosci 6:414–417.

Nakayama N, Okumura A, Shinoda J, Nakashima T, Iwama T (2006) Relationship between regional cerebral metabolism and consciousness disturbance in traumatic diffuse brain injury without large focal lesions: an FDG-PET study with statistical parametric mapping analysis. J Neurol Neurosurg Psychiatry 77:856–862.

Ojala M, Garriga GC (2010) Permutation tests for studying classifier performance. J Mach Learn Res 11:1833–1863.

Oostenveld R, Fries P, Maris E, Schoffelen J-M (2011) FieldTrip: open source software for advanced analysis of MEG. Comput Intell Neurosci 2011:156869.

Pal M (2005) Random forest classifier for remote sensing classification. Int J Remote Sens 26:217–222.

Park H-D, Tallon-Baudry C (2014) The neural subjective frame: from bodily signals to perceptual consciousness. Philos Trans R Soc Lond B Biol Sci 369:20130208.

Park H-D, Correia S, Ducorps A, Tallon-Baudry C (2014) Spontaneous fluctuations in neural responses to heartbeats predict visual detection. Nat Neurosci 17:612–618.

Park H-D, Bernasconi F, Bello-Ruiz J, Pfeiffer C, Salomon R, Blanke O (2016) Transient modulations of neural responses to heartbeats covary with bodily self-consciousness. J Neurosci 36:8453–8460.

Park H-D, Bernasconi F, Salomon R, Tallon-Baudry C, Spinelli L, Seeck M, Schaller K, Blanke O (2018) Neural sources and underlying mechanisms of neural responses to heartbeats, and their role in bodily self-consciousness: an intracranial EEG study. Cereb Cortex 28:2351–2364.

Raimondo F, Rohaut B, Demertzi A, Valente M, Engemann DA, Salti M, Fernandez Slezak D, Naccache L, Sitt JD (2017) Brain–heart interactions reveal consciousness in noncommunicating patients. Ann Neurol 82:578–591.

Riganello F, Chatelle C, Schnakers C, Laureys S (2018a) Heart rate variability as an indicator of nociceptive pain in disorders of consciousness? J Pain Symptom Manage 57:47–56.

Riganello F, Larroque SK, Bahri MA, Heine L, Martial C, Carrière M, Charland-Verville V, Aubinet C, Vanhaudenhuyse A, Chatelle C, Laureys S, Di PC (2018b) A heartbeat away from consciousness: heart rate variability entropy can discriminate disorders of consciousness and is correlated with resting-state fMRI brain connectivity of the central autonomic network. Front Neurol 9:769.

Rouder JN, Speckman PL, Sun D, Morey RD, Iverson G (2009) Bayesian t tests for accepting and rejecting the null hypothesis. Psychon Bull Rev 16:225–237.

Rudolf J, Ghaemi M, Ghaemi M, Haupt WF, Szelies B, Heiss WD (1999) Cerebral glucose metabolism in acute and persistent vegetative state. J Neurosurg Anesthesiol 11:17–24.

Schandry R, Sparrer B, Weitkunat R (1986) From the heart to the brain: a study of heartbeat contingent scalp potentials. Int J Neurosci 30:261–275.

Schiff ND (2015) Cognitive motor dissociation following severe brain injuries. JAMA Neurol 72:1413–1415.

Sel A, Azevedo RT, Tsakiris M (2017) Heartfelt self: cardio-visual integration affects self-face recognition and interoceptive cortical processing. Cereb Cortex 27:5144–5155.

Sergent C, Faugeras F, Rohaut B, Perrin F, Valente M, Tallon-Baudry C, Cohen L, Naccache L (2017) Multidimensional cognitive evaluation of patients with disorders of consciousness using EEG: a proof of concept study. Neuroimage Clin 13:455–469.

Sitt JD, King J-R, El Karoui I, Rohaut B, Faugeras F, Gramfort A, Cohen L, Sigman M, Dehaene S, Naccache L (2014) Large scale screening of neural signatures of consciousness in patients in a vegetative or minimally conscious state. Brain 137:2258–2270.

Song M, Yang Y, He J, Yang Z, Yu S, Xie Q, Xia X, Dang Y, Zhang Q, Wu X, Cui Y, Hou B, Yu R, Xu R, Jiang T (2018) Prognostication of chronic disorders of consciousness using brain functional networks and clinical characteristics. eLife 7:e36173.

Sperry R (1984) Consciousness, personal identity and the divided brain. Neuropsychologia 22:661–673.

Stender J, Gosseries O, Bruno M-A, Charland-Verville V, Vanhaudenhuyse A, Demertzi A, Chatelle C, Thonnard M, Thibaut A, Heine L, Soddu A, Boly M, Schnakers C, Gjedde A, Laureys S (2014) Diagnostic precision of PET imaging and functional MRI in disorders of consciousness: a clinical validation study. Lancet 384:514–522.

Stender J, Kupers R, Rodell A, Thibaut A, Chatelle C, Bruno M-A, Gejl M, Bernard C, Hustinx R, Laureys S, Gjedde A (2015) Quantitative rates of brain glucose metabolism distinguish minimally conscious from vegetative state patients. J Cereb Blood Flow Metab 35:58–65.

Steyerberg EW, Uno H, Ioannidis JPA, Calster B van, Ukaegbu C, Dhingra T, Syngal S, Kastrinos F (2018) Poor performance of clinical prediction models: the harm of commonly applied methods. J Clin Epidemiol 98:133–143.

Strobl C, Boulesteix A-L, Kneib T, Augustin T, Zeileis A (2008) Conditional variable importance for random forests. BMC Bioinformatics 9:307.

Tallon-Baudry C, Campana F, Park H-D, Babo-Rebelo M (2018) The neural monitoring of visceral inputs, rather than attention, accounts for first-person perspective in conscious vision. Cortex 102:139–149.

Task Force of the European Society of Cardiology the North American Society of Pacing (1996) Heart rate variability: standards of measurement, physiological interpretation, and clinical use. Circulation 93:1043–1065.

Thayer JF, Peasley C, Muth ER (1996) Estimation of respiratory frequency from autoregressive spectral analysis of heart period. Biomed Sci Instrum 32:93–99.

Thibaut A, Bruno M-A, Chatelle C, Gosseries O, Vanhaudenhuyse A, Demertzi A, Schnakers C, Thonnard M, Charland-Verville V, Bernard C, Bahri M, Phillips C, Boly M, Hustinx R, Laureys S (2012) Metabolic activity in external and internal awareness networks in severely brain-damaged patients. J Rehabil Med 44:487–494.

Tobaldini E, Toschi-Dias E, Trimarchi PD, Brena N, Comanducci A, Casarotto S, Montano N, Devalle G (2018) Cardiac autonomic responses to nociceptive stimuli in patients with chronic disorders of consciousness. Clin Neurophysiol 129:1083–1089.

Tommasino C, Grana C, Lucignani G, Torri G, Fazio F (1995) Regional cerebral metabolism of glucose in comatose and vegetative state patients. J Neurosurg Anesthesiol 7:109–116.

Tsuchiya N, Wilke M, Frässle S, Lamme VAF (2015) No-report paradigms: extracting the true neural correlates of consciousness. Trends Cogn Sci 19:757–770.

Tzourio-Mazoyer N, Landeau B, Papathanassiou D, Crivello F, Etard O, Delcroix N, Mazoyer B, Joliot M (2002) Automated anatomical labeling of activations in SPM using a macroscopic anatomical parcellation of the MNI MRI single-subject brain. NeuroImage 15:273–289.

van Veluw SJ, Chance SA (2014) Differentiating between self and others: an ALE meta-analysis of fMRI studies of self-recognition and theory of mind. Brain Imaging Behav 8:24–38.

Verikas A, Gelzinis A, Bacauskiene M (2011) Mining data with random forests: a survey and results of new tests. Pattern Recognit 44:330–349.

Wannez S, Heine L, Thonnard M, Gosseries O, Laureys S (2017) The repetition of behavioral assessments in diagnosis of disorders of consciousness. Ann Neurol 81:883–889.

Woo C-W, Chang LJ, Lindquist MA, Wager TD (2017) Building better biomarkers: brain models in translational neuroimaging. Nat Neurosci 20:365–377.

Yarkoni T, Poldrack RA, Nichols TE, Van Essen DC, Wager TD (2011) Large-scale automated synthesis of human functional neuroimaging data. Nat Methods 8:665–670.